

# Testing the unitarity of the light neutrino mixing matrix

E. Gabrielli<sup>a,b,c</sup>, A. Lind<sup>d</sup>, L. Marzola<sup>c,e</sup>, K. Mürsepp<sup>c,d</sup>, E. Nardi<sup>c,d</sup>

<sup>a</sup> *Physics Department, University of Trieste, Strada Costiera 11, I-34151 Trieste, Italy*

<sup>b</sup> *INFN, Sezione di Trieste, Via Valerio 2, I-34127 Trieste, Italy*

<sup>c</sup> *Laboratory of High-Energy and Computational Physics, NICPB, Rävåla 10, 10143 Tallinn, Estonia*

<sup>d</sup> *INFN, Laboratori Nazionali di Frascati, C.P. 13, 100044 Frascati, Italy*

<sup>e</sup> *Institute of Computer Science, University of Tartu, Narva mnt 18, 51009 Tartu, Estonia*

We propose a novel test of the unitarity of the Pontecorvo–Maki–Nakagawa–Sakata (PMNS) mixing matrix at collider experiments. Our approach exploits the incomplete cancellation between  $t$ -channel neutrino exchange and  $s$ -channel gauge-boson contributions that arises in the presence of violation of the flavor-diagonal PMNS unitarity conditions, leading to an anomalous growth of the cross section with energy. Such effects are generic in extensions of the Standard Model in which light neutrinos mix with heavier states, and can manifest at colliders as long as the characteristic energy of the process remains below the mass threshold of the new degrees of freedom. After briefly reviewing these scenarios, we employ our strategy to derive model-independent bounds on flavor diagonal unitarity-violating effects using LEP II data. We then present sensitivity projections for future lepton and hadron colliders, demonstrating that they are well suited to probe the unitarity of the neutrino mixing matrix with this method.

## I. INTRODUCTION

In order to explain the suppression of neutrino masses, the Standard Model (SM) is often extended with additional neutral fermions generally assumed to be heavier than the electroweak scale. In a theory presenting  $n$  additional states on top of the three SM neutrinos, the mass matrix of the neutral fermions has the following structure:

$$\mathcal{M} = \begin{pmatrix} \mathcal{M}_{33} & \mathcal{M}_{3n} \\ \mathcal{M}_{n3} & \mathcal{M}_{nn} \end{pmatrix}, \quad (1)$$

where  $\mathcal{M}_{33}$  and  $\mathcal{M}_{nn}$  are symmetric matrices, and  $\mathcal{M}_{n3} = \mathcal{M}_{3n}^T$ . The complex-symmetric matrix  $\mathcal{M}$  can be expressed via Takagi factorisation as  $\mathcal{M} = U^* \hat{M} U^\dagger$ , where  $\hat{M}$  is a real diagonal matrix whose diagonal elements are the nonnegative square roots of the eigenvalues of  $\mathcal{M}^\dagger \mathcal{M} = U \hat{M}^2 U^\dagger$ , and  $U$  is a unitary matrix ( $U^\dagger = U^{-1}$ ). The mass eigenvalues in  $\hat{M}$  can be sorted into two sets: one containing the three masses of the light SM neutrinos,  $\hat{m}_{\nu_i}$  with  $i = 1, 2, 3$ , and one comprising the masses  $\hat{M}_{\mathcal{N}_n}$  of the  $n$  additional heavy neutral fermions  $\mathcal{N}_n$ . The unitary matrix  $U$  can be written in block form as

$$U = \begin{pmatrix} U_\nu & U_{3n} \\ U_{n3} & U_{nn} \end{pmatrix}, \quad (2)$$

where  $U_\nu$  describes the superposition of the light neutrinos mass eigenstates  $\nu_i$  in the active neutrino state of flavor  $\alpha$

$$|\nu^\alpha\rangle = \sum_{i=1}^3 (U_\nu^*)^{\alpha i} |\nu_i\rangle + \sum_{k=1}^n (U_{3n}^*)^{\alpha k} |\mathcal{N}_k\rangle, \quad (3)$$

and is commonly denoted as the Pontecorvo–Maki–Nakagawa–Sakata (PMNS) [1, 2] matrix.<sup>1</sup> In the presence of mixing between the light neutrinos and the heavy neutral fermions, the SM leptonic charged current Lagrangian is modified as

$$\mathcal{L} = -\frac{g}{\sqrt{2}} W_\mu^- \bar{\ell}_\alpha \gamma^\mu (U_\nu^{\alpha i} \nu_i + U_{3n}^{\alpha i} \mathcal{N}_i) + H.c. \quad (4)$$

with  $\ell_\alpha$ ,  $\alpha = (e, \mu, \tau)$ , being the vector of the left-handed (LH) SM charged leptons, and with  $U_{3n}$  accounting for the new heavy  $\mathcal{N}_i$  components in  $\nu_\alpha$ . Imposing the unitarity of the matrix  $U$  straightforwardly implies deviations from unitarity for the PMNS matrix:

$$\sum_{i=1}^3 |U_\nu^{\alpha i}|^2 = 1 - \sum_{i=4}^n |U_{3n}^{\alpha i}|^2 = 1 - \delta_\alpha, \quad (5)$$

$$\sum_{i=1}^3 U_\nu^{\alpha i} U_\nu^{\beta i *} = - \sum_{i=4}^n U_{3n}^{\alpha i} U_{3n}^{\beta i *} = \epsilon_{\alpha\beta} \quad (\beta \neq \alpha). \quad (6)$$

The parameters  $\epsilon_{\alpha\beta}$  ( $\alpha, \beta = e, \mu, \tau$ ) in Eq. (6) are responsible for enhancing lepton flavor violating (LFV) transitions such as  $\mu \rightarrow e\gamma$ ,  $\tau \rightarrow \mu\gamma$  and  $\tau \rightarrow e\gamma$ , with respect to the SM rates. Experimental bounds on these rare processes are particularly strong, and provide constraints at the level of  $|\epsilon_{\mu e}| \lesssim 10^{-5}$  and  $|\epsilon_{\tau\mu}|, |\epsilon_{\tau e}| \lesssim 6 \times 10^{-3}$  [3–5]. The parameters  $\delta_\alpha \geq 0$  ( $\alpha = e, \mu, \tau$ ) in Eq. (5) are responsible for flavor diagonal non-unitarity effects. They are constrained by global fits to high precision electroweak data at the level of  $\delta_e \lesssim 2 \times 10^{-3}$ ,  $\delta_\mu \lesssim 2 \times 10^{-4}$  and  $\delta_\tau \lesssim 5 \times 10^{-3}$  [4–7].

An interesting way to test diagonal non-unitarity effects sourced by the PMNS matrix is to search for processes in which such effects may spoil perturbative unitarity of certain cross sections in high energy collisions.

<sup>1</sup> We work in the flavor basis, wherein the mass matrix of the charged leptons is diagonal with real nonnegative entries.

A particularly promising environment is then provided by the lepton–antilepton colliders, and, to some degree, by the upcoming High-Luminosity (HL) phase of the LHC experiment. Indeed, as long as the energy of the process remains below the scale of the heavy neutral fermion masses, non-unitarity effects can induce an anomalous energy scaling of the cross section in interactions involving the exchange of the light neutrinos. The effect can then be investigated at hadron colliders via the  $W^+W^-$  fusion, and at lepton colliders via the  $W^+W^-$  production. The same underlying mechanism has been recently exploited to test the unitarity of the Cabibbo–Kobayashi–Maskawa quark mixing matrix, by studying the anomalous growth of the  $pp \rightarrow W^+W^-$  cross section at the LHC, and at various future hadron colliders [8].

Assessing how accurately the proposed method can constrain non-unitarity effects in the neutrino mixing with the available data, as well as with measurements at future  $pp$ ,  $e^+e^-$  and  $\mu^+\mu^-$  colliders, is the main goal of this work. To this purpose, in the next section, we examine the theoretical expectations for the size of the parameters  $\delta_\alpha$  in well-motivated neutrino mass models. Subsequently, we derive bounds on  $\delta_\alpha$  from the available LEP data, as well as for the projected sensitivity of the future high-energy facilities such as HL-LHC, FCC-ee, FCC-hh, CLIC, ILC and the muon collider. Our conclusions are presented in the final section.

## II. NEUTRINO MASS MODELS AND PMNS NON-UNITARITY

**Type I seesaw.** In the type I seesaw model [9–12], three heavy singlet Majorana fermions  $N_R = (N_1, N_2, N_3)$  are added to the SM. Consequently, the matrices  $\mathcal{M}$  in Eq. (1) and  $U$  in Eq. (2) have dimension  $6 \times 6$ .<sup>2</sup> In the basis  $(\nu_L, N_R^c)$  with  $\nu_L = (\nu_e, \nu_\mu, \nu_\tau)$  the mass matrix has the following structure:

$$\mathcal{M}_{T1} = \begin{pmatrix} 0 & m_D \\ m_D^T & \hat{M} \end{pmatrix}, \quad (7)$$

where  $\hat{M}$  is a matrix of Majorana masses that, with a proper choice of basis, can be taken as diagonal. The matrix  $m_D$ , proportional to the Higgs boson vacuum expectation value (vev), hosts the Dirac masses. The suppression of the light neutrino masses is obtained under the natural assumption that all the entries in the  $3 \times 3$  matrix  $\theta = m_D \hat{M}^{-1}$  are  $\ll 1$ . In this limit, the light neutrino mass matrix is given by

$$m_\nu = V_L^* \hat{m}_\nu V_L^\dagger \simeq -m_D \frac{1}{\hat{M}} m_D^T, \quad (8)$$

where  $\hat{m}_\nu = \text{diag}(m_1, m_2, m_3)$  and  $V_L$  is a unitary matrix. Note that  $V_L$  differs from the exact (non-unitary) light neutrino mixing matrix  $U_\nu$  by terms of  $O(m_D^2/\hat{M}^2)$ . It is easily seen that, after neglecting the unphysical minus sign, the last expression is reproduced by writing  $m_D$  in the Casas-Ibarra (CI) parametrisation [16] as

$$m_D = V_L^* \hat{m}_\nu^{\frac{1}{2}} R^T \hat{M}^{\frac{1}{2}}, \quad (9)$$

provided that  $R$  is an arbitrary complex  $3 \times 3$  orthogonal matrix and that the Yukawa couplings  $Y$  determining the Dirac mass matrix  $m_D = Yv$  are perturbative.<sup>3</sup>

At the leading order in  $\theta$  the complete mixing matrix that diagonalises  $\mathcal{M}_{T1}$  in Eq. (7) is given by [18]

$$U \simeq \begin{pmatrix} 1 - \frac{1}{2}\theta\theta^\dagger & \theta \\ -\theta^\dagger & 1 - \frac{1}{2}\theta^\dagger\theta \end{pmatrix}, \quad (10)$$

and hence, in type I seesaw models, the deviation from unitarity in Eq. (5) is given by

$$\delta_\alpha = \sum_{i=4}^6 |\theta_{\alpha i}|^2, \quad (11)$$

in which, by using Eq. (9), the light-heavy mixing matrix can be written as

$$\theta = V_L^* \sqrt{\hat{m}_\nu} R^T \frac{1}{\sqrt{\hat{M}}}. \quad (12)$$

Can some of the parameters  $\delta_\alpha$  of the type I seesaw be sufficiently large to be observable? In principle, yes. However, taking as an order of magnitude estimate  $\hat{m}_\nu \sim O(0.1 \text{ eV})$  and  $\hat{M} \sim O(400 \text{ GeV})$  (for the consistency of the seesaw approximation, the lowest possible values for the entries in  $\hat{M}$  cannot be below the electroweak scale), we see that violation of unitarity at the level of  $\delta_\alpha \sim 10^{-4}$  can be ensured only if some entries in the matrix  $R$  exceed  $O(10^4)$ . Clearly, this requirement implies a certain amount of fine-tuning, in particular in the structure of the Dirac mass matrix  $m_D$  (see Eq. (9)).

**Inverse seesaw and double seesaw models.** In the inverse seesaw (IS) [19] and double seesaw (DS) [20] models, two triplets of SM singlet fermions  $N_R = (N_1, N_2, N_3)$  and  $S_L = (S_1, S_2, S_3)$  are introduced. The mass matrix for the neutral states is  $9 \times 9$  and, in the basis  $\mathcal{N} = (\nu_L, N_R^c, S_L)$ , has the following structure:

$$\mathcal{M}_{IS,DS} = \begin{pmatrix} 0 & m_D^T & 0 \\ m_D & 0 & M \\ 0 & M^T & \hat{\mu} \end{pmatrix} = \begin{pmatrix} 0 & \mathbb{M}_D^T \\ \mathbb{M}_D & \mathbb{M} \end{pmatrix}, \quad (13)$$

<sup>2</sup> A minimal version of the type I seesaw, consistent with all current neutrino data and predicting a massless lightest neutrino, can be obtained by adding only two new neutral fermions [13–15].

<sup>3</sup> The matrix  $R$  can be parametrised, for example, as  $R = \text{diag}(\pm 1, \pm 1, \pm 1) R^{(23)} R^{(13)}(z_{13}) R^{(12)}(z_{12})$ , with  $R^{(ij)}$  being a rotation matrix acting in the  $(ij)$  plane with a complex angle  $z_{ij}$  [16, 17].

where, in the second expression,

$$\mathbb{M}_D = \begin{pmatrix} m_D \\ 0 \end{pmatrix}, \quad \mathbb{M} = \begin{pmatrix} 0 & M \\ M^T & \hat{\mu} \end{pmatrix}. \quad (14)$$

Without loss of generality, the Majorana mass term  $\bar{S}_L^c \hat{\mu} S_L$  in Eqs. (13) and (14) can be taken as diagonal by a field redefinition of the  $S_L$  neutral fermions. The matrix  $M$  that couples  $N_R$  and  $S_L$  can be factorised as  $U_R \hat{M} W_L^\dagger$ , with  $\hat{M}$  diagonal with real non-negative entries. The unitary matrix  $U_R$  can then be absorbed in a redefinition of the  $N_R$  fields, while the unitary matrix  $W_L$  is defined in terms of three real and three imaginary physical parameters [21].

The mass matrix  $\mathcal{M}_{IS,DS}$  can result in a suppression of the active neutrino masses if suitable hierarchies among its entries are assumed. The IS model assumes  $\hat{\mu} \ll m_D \ll M$ , so that an approximate diagonalisation yields the light neutrino mass matrix

$$m_\nu = V_L^* \hat{m}_\nu V_L^\dagger \simeq -\mathbb{M}_D^T \frac{1}{\mathbb{M}} \mathbb{M}_D = m_D^T \frac{1}{M^T} \hat{\mu} \frac{1}{M} m_D. \quad (15)$$

This equation shows that a suppression of the light neutrino masses can be obtained thanks to small values of the lepton number violating (LNV) entries in  $\hat{\mu}$ , without the need for exceedingly small values of the ratio  $m_D/M$ . Consequently, the  $N_R$  masses could quite naturally fall within experimental reach. Adopting a CI-like parametrisation in the IS model, we have:

$$m_D = M \frac{1}{\sqrt{\hat{\mu}}} R \sqrt{\hat{m}_\nu} V_L^\dagger. \quad (16)$$

After diagonalisation, the  $N_R$  and  $S_L$  states give rise to a pair of heavy quasi-Dirac neutrinos  $N_\pm$  with masses of  $O(M)$  and a characteristic splitting of  $O(\hat{\mu}) \ll O(M)$ . The mixing between the light and heavy sectors is regulated by the block diagonal  $1 \times 2$  matrix

$$\theta = \mathbb{M}_D^T \frac{1}{\mathbb{M}} = \left( -m_D^T \frac{1}{M^T} \hat{\mu} \frac{1}{M}, m_D^T \frac{1}{M^T} \right). \quad (17)$$

Given that the ratio  $\hat{\mu} \frac{1}{M}$  is a suppression factor within the IS model, the leading contribution to the PNMS unitarity violation in  $\theta\theta^\dagger$  is given by the second block, that, with a slight abuse of notation, we denote  $\theta_{12}$ . We have

$$\theta_{12} \simeq m_D^T \frac{1}{M^T} = V_L^* \sqrt{\hat{m}_\nu} R^T \frac{1}{\sqrt{\hat{\mu}}}, \quad (18)$$

which, notably, is not suppressed by the large scale  $M$ . Taking  $\hat{m}_\nu \sim O(0.1 \text{ eV})$  and  $\hat{\mu} \sim O(100 \text{ keV})$ , we see that it would be sufficient to have entries of  $O(10)$  in  $R$  to generate a violation of unitarity at the level of  $\delta_\alpha \sim 10^{-4}$ .

The DS model assumes for the entries in the mass matrix in Eq. (13) the hierarchy  $\hat{\mu} \gg M \gg m_D$ . The expression for the light neutrino mass matrix given in Eq. (15) and the CI-like parametrisation in Eq. (16) remain valid

also in this case. However, in the DS model,  $\hat{\mu} \frac{1}{M}$  represents an enhancement factor and so the leading term sourcing the PNMS unitarity violation in  $\theta\theta^\dagger$  is the first block in Eq. (17)

$$\theta_{11} = m_D^T \frac{1}{M^T} \hat{\mu} \frac{1}{M} = V_L^* \sqrt{\hat{m}_\nu} R^T \sqrt{\hat{\mu}} \frac{1}{M}, \quad (19)$$

which is enhanced by a factor  $\sqrt{\hat{\mu}/M} \gg 1$  with respect to the type 1 seesaw case.

**Linear seesaw model.** Another model that can be realised with new degrees of freedom at a low scale is the linear seesaw (LS) model [22, 23], which involves the same number of additional neutral fermions as in the previous case. In the basis  $(\nu_L, N_R^C, S_L)$ , the mass matrix reads

$$\mathcal{M}_{LS} = \begin{pmatrix} 0 & m_D^T & m_L^T \\ m_D & 0 & M \\ m_L & M^T & \hat{\mu} \end{pmatrix}, \quad (20)$$

where the non-zero 31 entries  $m_L$  are generated by the vev of a Higgs doublet similarly to  $m_D$  and, thus, are naturally of the order of the weak scale. Assuming the hierarchy  $m_L, m_D \ll M$ , an approximate diagonalisation performed as in Eq. (13), with  $\mathbb{M}_D^T = (m_D^T, m_L^T)$ , yields

$$m_\nu \simeq m_D \frac{1}{M^T} \hat{\mu} \frac{1}{M} m_D - m_L^T \frac{1}{M} m_D - m_D^T \frac{1}{M^T} m_L. \quad (21)$$

Note that if  $\hat{\mu} \rightarrow 0$ , the expression becomes linear in the active neutrino Yukawa couplings  $Y = m_D/v$  to the right-handed neutrinos  $N_R$ , hence the name *linear seesaw*. The matrix

$$\theta = \mathbb{M}_D^T \frac{1}{\mathbb{M}} = \left( -m_D^T \frac{1}{M^T} \hat{\mu} \frac{1}{M} + m_L^T \frac{1}{M}, m_D^T \frac{1}{M^T} \right) \quad (22)$$

controls the mixing between the light and heavy sectors of the theory.

A CI-like parametrisation can be written down also for the LS model [24, 25], however, it has a block matrix form that renders the expressions for the deviations from unitarity more complicated. From Eq. (22) we can see that the unitarity violation parameter given by  $\theta\theta^\dagger$  contains three additional terms besides the ones in Eq. (18) and Eq. (19), of which two are a pair of Hermitian conjugate combinations [26]. All in all, the expected order of magnitude of unitarity violation is given by

$$\theta\theta^\dagger \sim O \left[ \frac{m_D^2}{M^2} \left( 1 + \frac{m_L^2}{m_D^2} + \frac{m_L}{m_D} \frac{\hat{\mu}}{M} + \frac{\hat{\mu}^2}{M^2} \right) \right]. \quad (23)$$

Which of these terms will dominate depends on the specific choice of the model parameters. Assuming, for example, that the terms containing  $\hat{\mu}$  are negligible, the violation of unitarity is determined by terms of order  $(m_D^2 + m_L^2)/M^2$ , and can be sizable if  $m_D$  or  $m_L$  are not much smaller than  $M$ .

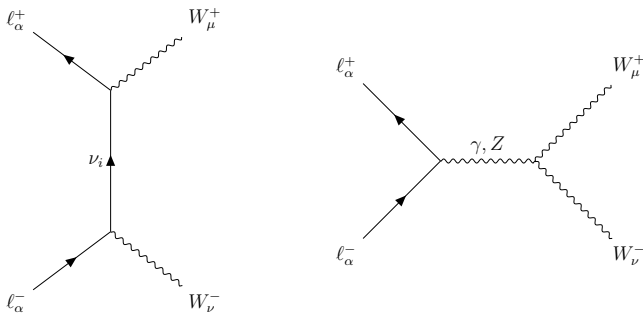


FIG. 1. Tree level Feynman diagrams for the processes  $\ell_\alpha^+ \ell_\alpha^- \rightarrow W^+ W^-$ ,  $\alpha = e, \mu, \tau$ . As explained in the text, the Higgs boson contribution is neglected. The arrows on the fermion lines indicate the momentum flow.

### III. UNITARITY VIOLATION AT LEPTON COLLIDERS

The violation of unitarity in the PMNS matrix is expected to break perturbative unitarity at the amplitude level in the process<sup>4</sup>

$$\ell_\alpha^+(p_1) \ell_\alpha^-(p_2) \rightarrow W^+(k_1) W^-(k_2), \quad (24)$$

where  $\alpha = e, \mu, \tau$  label the initial state leptons. In the SM, this process proceeds via  $s$ -channels mediated by the Higgs boson,  $Z$  boson, and photon, and via  $t$ -channel involving the exchange of the neutrinos mass-eigenstates  $\nu_i$ . The corresponding tree-level Feynman diagrams are shown in Fig. 1. In order to assess the power of lepton colliders to constrain non-unitarity effects, we restrict ourselves to consider electron and muon initial states, and work in the limit where the corresponding masses vanish—as justified by the typical energy of the processes we consider. In this limit we then neglect the Higgs boson  $s$ -channel contribution. We can then write the amplitude for  $\ell_\alpha^+ \ell_\alpha^- \rightarrow W^+ W^-$  as:

$$\mathcal{M}_\alpha = \mathcal{M}_\alpha^t + \mathcal{M}_\alpha^s. \quad (25)$$

where  $\mathcal{M}_\alpha^t$  and  $\mathcal{M}_\alpha^s$  represent the  $s$ -channel and  $t$ -channel amplitudes, respectively. The potential presence in  $\mathcal{M}_\alpha^t$  of terms spoiling the PMNS matrix unitarity prevents the exact cancellation of the terms proportional to the final state momenta contained in the two amplitudes, which gauge invariance otherwise ensures.

In order to expose the origin of these terms, consider the  $t$ -channel contribution corresponding to diagram (a) in Fig. 1. We have

$$\mathcal{M}_\alpha^t = \sum_{i=1}^3 |U_\nu^{\alpha i}|^2 \mathcal{M}_i^t \simeq \mathcal{M}_\nu^t \sum_{i=1}^3 |U_\nu^{\alpha i}|^2, \quad (26)$$

<sup>4</sup> The first computation of the related tree-level cross section can be found in Ref. [27]. Radiative corrections to the process were first discussed in Refs. [28–30].

where the second equality holds once neutrino mass square differences are neglected so that  $\mathcal{M}_i^t = \mathcal{M}_\nu^t$  can be factored out from the sum. If the PMNS mixing matrix is unitary, then

$$\sum_{i=1}^3 |U_\nu^{\alpha i}|^2 = 1, \quad (27)$$

holds for each row  $\alpha$ .

In frameworks where the SM neutral fermion sector is enlarged by adding  $n$  new states that mix with the SM neutrinos, as in the neutrino mass models reviewed in Section II, unitarity holds for the full  $(3+n) \times (3+n)$  matrix  $U$ . However, if the characteristic mass scale of the heavy neutrinos lies well above the typical energy at which the  $W$  boson pair production is probed, the  $t$ -channel diagrams involving their exchange are effectively negligible. The sum over  $t$ -channel contributions is therefore restricted to the three light propagating degrees of freedom, whose mixing terms do not saturate the unitarity relation, see Eq. (5). The quantities  $\delta_\alpha$  defined in Eq. (5) thus parametrize the deviation from unitarity for the specific initial state lepton  $\alpha = e, \mu, \tau$ . As we will show below, this deviation spoils the cancellation of  $s$ - and  $t$ -channel contributions, thereby resulting in an anomalous growth of the cross section as long as the energy remains below the mass scales of the new states.

The amplitude in Eq.(25) can be compactly written as

$$\mathcal{M}_\alpha = -ie^2 \left[ \bar{v}(p_1) \Gamma_\alpha^{\mu\nu} u(p_2) \right] \varepsilon_\mu^*(k_1) \varepsilon_\nu^*(k_2), \quad (28)$$

where we indicated with  $\varepsilon_\mu(k_1)$  and  $\varepsilon_\nu(k_2)$  the polarisation vectors of the  $W^+$  and  $W^-$ , respectively. The effective vertex  $\Gamma_\alpha^{\mu\nu}$  is given under the approximation of massless initial state by

$$\Gamma_{\alpha=e,\mu,\tau}^{\mu\nu} = \frac{1}{s} (\gamma_\beta \bar{g}_V - \gamma_\beta \gamma_5 \bar{g}_A) V^{\beta\nu\mu}(k_1 + k_2, -k_2, -k_1) + \frac{\xi_\alpha}{4ts_w^2} \gamma^\nu (\not{p}_2 - \not{k}_2) \gamma^\mu (1 - \gamma_5), \quad (29)$$

with  $s_w = \sin \theta_W$ ,  $\theta_W$  being the Weinberg angle, and  $e$  the unit electric charge.

The flavor universal effective couplings  $\bar{g}_{V,A}$  in Eq. (29) are given by

$$\bar{g}_V = -1 + \frac{g_V \chi}{s_w^2}, \quad \bar{g}_A = \frac{g_A \chi}{s_w^2}, \quad \chi = \frac{s}{2(s - M_Z^2)}, \quad (30)$$

where  $M_Z$  is the  $Z$  boson mass,  $g_V = -\frac{1}{2} + 2s_w^2$ ,  $g_A = -\frac{1}{2}$ . The  $\chi$  term in Eq. (30), which weights the contribution of the virtual  $Z$  channel, is real since we neglect the  $Z$  width contribution. The function  $V_{\beta\nu\mu}(k_1, k_2, k_3)$  arises from the Feynman rule for the trilinear vertex  $V_\beta(k_1) W_\nu^+(k_2) W_\mu^-(k_3)$ , with  $V \in \{\gamma, Z\}$ , and is given by

$$V_{\beta\nu\mu}(k_1, k_2, k_3) = (k_1 - k_2)_\mu g_{\beta\nu} + (k_2 - k_3)_\beta g_{\mu\nu} + (k_3 - k_1)_\nu g_{\beta\mu}, \quad (31)$$

for incoming momenta:  $k_1 + k_2 + k_3 = 0$ . The Mandelstam variables  $s$  and  $t$  appearing in the above equations are given by

$$s = (p_1 + p_2)^2, \quad t = (p_2 - k_2)^2. \quad (32)$$

The square amplitude for the process  $\ell_\alpha^+ \ell_\alpha^- \rightarrow W^+ W^-$ , averaged over the initial state spins and summed over the final state polarisations, can be written as

$$|\overline{\mathcal{M}}_\alpha|^2 = |\overline{\mathcal{M}}^{\text{SM}}|^2 + \delta_\alpha \Delta_1 + \delta_\alpha^2 \Delta_2, \quad (33)$$

where  $|\overline{\mathcal{M}}_\alpha^{\text{SM}}|^2$  is the SM contribution and the extra terms vanish in absence of unitarity violation.

By retaining only the leading orders in the  $s/M_W^2 \gg 1$  expansion, with  $M_W$  the  $W$  boson mass, we find

$$\begin{aligned} \Delta_1 &\simeq -\frac{\alpha_w^2 \pi^2}{2} \left( \frac{s}{M_W^2} \right) s_\Theta^2 \left[ 2 - \frac{M_Z^2}{M_W^2} (1 - 2s_W^2) \right], \\ \Delta_2 &\simeq \frac{\alpha_w^2 \pi^2}{4} \left[ \left( \frac{s^2}{M_W^4} \right) s_\Theta^2 + \left( \frac{s}{M_W^2} \right) 4(3 + c_\Theta^2) \right], \end{aligned} \quad (34)$$

with  $\alpha_w = e^2/(4\pi s_W^2)$  and  $s_W^2$  denoting the sine square of the electroweak angle, while  $c_\Theta = \cos \Theta$  and  $s_\Theta = \sin \Theta$ , with  $\Theta$  being the scattering angle between the  $e^+$  and  $W^+$  momenta. Notice that the correction  $\delta_\alpha \Delta_1 \propto -\delta_\alpha s$ , is always negative, while  $\delta_\alpha^2 \Delta_2$ , that contains a term  $\propto \delta_\alpha^2 s^2$ , is always positive. Thus, for small  $\delta_\alpha$ , the unitarity violation effects will suppress the cross section at low energies with respect to the SM. However, for any given value of  $\delta_\alpha$  there will be a certain value of the center-of-mass energy  $s$  for which the  $\delta_\alpha^2 \Delta_2$  correction starts dominating, and the cross section will then overshoots the SM prediction. This behavior is clearly illustrated in Fig. 2. For the sake of the present analysis, we have used the exact expressions of the  $\Delta \mathcal{M}_1$  and  $\Delta \mathcal{M}_2$  terms, which are given in Appendix A.

The differential cross section for the process reads:

$$\left( \frac{d\sigma_\alpha}{d\Omega} \right) = \frac{\beta_w}{64\pi^2 s} |\overline{\mathcal{M}}_\alpha|^2, \quad (35)$$

where  $\beta_w = \sqrt{1 - 4M_W^2/s}$  is the  $W$  boson velocity in the center of mass frame.

In Fig. 2 we plot the ratio of the total cross section Eq. (35) for the two values  $\delta_\alpha = 0.1$  and  $\delta_\alpha = 0.01$ , relative to the SM prediction (corresponding to  $\delta_\alpha = 0$ ), as a function of  $\sqrt{s}$ . If a deviation from unity is measured for this ratio, this could be straightforwardly interpreted as the effect of unitarity-breaking in the lepton mixing matrix. As the center-of-mass energy reaches the mass scale of these new states, the cross section starts to fall with increasing energy. In the following sections, we exploit the deviations induced by the  $\delta_\alpha$  parameters to assess the sensitivity of collider experiments to the unitarity violation effects they imply.

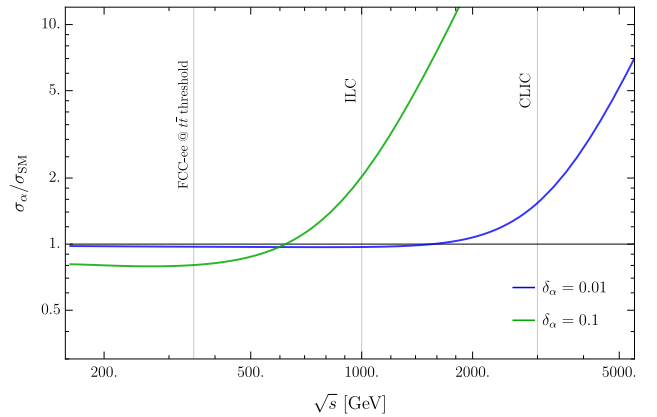


FIG. 2. The ratio of the total cross section including the NP contributions (Eq. (35)) for  $\delta_\alpha = 0.01$  (blue solid line) and  $\delta_\alpha = 0.1$  (green solid line), relative to the SM prediction ( $\delta_\alpha = 0$ ) as a function of the center of mass energy.

#### IV. LEPTON COLLIDER BOUNDS ON $\delta_\alpha$

In order to investigate the power of lepton colliders to constrain the diagonal unitarity violating effects encoded in the  $\delta_\alpha$  parameters, we set up  $\chi^2$  tests that highlight the parameter ranges allowed at 95% confidence level (CL).

Starting with LEP II, we utilise the measurements [31] reported in Tab. I of the  $e^+e^- \rightarrow W^+W^-$  cross section,  $\sigma_i$ , and the relative experimental errors,  $\epsilon_i$ , where the subscript  $i = 1, 2, \dots, 6$  denotes the six different center of mass energies  $\sqrt{s_i}$  at which the measurements were performed.

$\sqrt{s_i}$ [GeV]	$ \sigma_i$ [pb]	$ \epsilon_i$ [pb]
183	15.83	0.36
189	16.05	0.22
192	16.80	0.50
196	17.39	0.35
200	16.91	0.32
202	17.11	0.46

TABLE I. LEP II data used for the  $\chi^2$  analysis with six degrees of freedom.

The  $\chi^2$  test we use is then given by

$$\chi^2 = \sum_{i=1}^6 \left( \frac{\sigma_i - \frac{\sigma_i}{\sigma_{\text{SM}}(s_i)} \sigma_e(s_i)}{\epsilon_i} \right)^2 \leq 12.592, \quad (36)$$

where  $\sigma_e$  is the tree-level cross section for the  $e^+e^- \rightarrow W^+W^-$  process, including effects of violation of PMNS unitarity ( $\delta_e \neq 0$ ),  $\sigma_{\text{SM}} \equiv \sigma_e(\delta_e = 0)$  is the SM cross section, and  $\sigma_i/\sigma_{\text{SM}}(s_i)$  is a rescaling factor that effectively accounts for next-to-leading order (NLO) corrections, experimental cuts, and detector efficiencies. The resulting bound on  $\delta_e$  that accounts for unitarity violations in the

first row of the PMNS matrix is

$$\delta_e \lesssim 0.0135 \quad (\text{LEP II}), \quad (37)$$

at 95% CL.

To forecast a possible bound obtainable at the FCC-ee, we perform a  $\chi^2$ -test targeting the projected number of events expected at the center of mass energy of  $\sqrt{s} = 350$  GeV with a benchmark luminosity of  $\mathcal{L} = 1.8 \text{ ab}^{-1}$ , corresponding to 5 years of operation [32, 33]. We obtain:

$$\chi^2 = \frac{(N_{\text{obs}} - N_{\text{exp}})^2}{N_{\text{exp}}} = \mathcal{L} \frac{(\sigma_e - \sigma_{\text{SM}})^2}{\sigma_{\text{SM}}} \leq 3.841, \quad (38)$$

where we have taken into account only the statistical error. Systematic errors related to the setup of the experiment, as well as the contribution to the overall uncertainty of yet unknown higher order corrections are expected to be important, although one can hope that, by the time the measurement will be performed, these uncertainties will eventually be reduced at a level not exceeding the statistical error.

With this assumption, we obtain for the 95% CL limit achievable at the FCC-ee, the following projection:

$$\delta_e \lesssim 1.6 \times 10^{-4} \quad (\text{FCC-ee}). \quad (39)$$

We remark that even if the effects of PMNS unitarity violation on the cross section generally grow with the energy, the FCC-ee bound is primarily due to the extremely high luminosity of the machine, which enhances the sensitivity of the process to the anomalous  $\delta_e$  effect, even for a center of mass energy not far above the electroweak scale. Future  $e^+e^-$  linear colliders and/or muon colliders, which are designed to run at center of mass energies well above the TeV scale, will be able to probe genuine high-energy effects due to, respectively,  $\delta_e$  and  $\delta_\mu$ . In particular, we consider the cases of the future  $e^+e^-$  International Linear Collider (ILC) [34–36] and Compact Linear Collider (CLIC) [37–39], respectively expected to run at 1 TeV for an integrated luminosity of  $8 \text{ ab}^{-1}$ , and at 3 TeV for an integrated luminosity of  $5 \text{ ab}^{-1}$ . Repeating the previous analysis we then find

$$\begin{aligned} \delta_e &\lesssim 9.6 \times 10^{-5} \quad (\text{ILC}), \\ \delta_e &\lesssim 9.1 \times 10^{-5} \quad (\text{CLIC}), \end{aligned} \quad (40)$$

at a 95% CL. For the muon collider, we consider two possible benchmark points: BM1 with  $\sqrt{s} = 3 \text{ TeV}$  and  $\mathcal{L} = 1 \text{ ab}^{-1}$ , and BM2 with  $\sqrt{s} = 10 \text{ TeV}$  and  $\mathcal{L} = 10 \text{ ab}^{-1}$  [40]. In these cases, assuming as before that statistical errors dominate, we obtain at 95% CL:

$$\begin{aligned} \delta_\mu &\lesssim 2.2 \times 10^{-4} \quad (\text{BM1}), \\ \delta_\mu &\lesssim 3.1 \times 10^{-5} \quad (\text{BM2}). \end{aligned} \quad (41)$$

To conclude the section, we mention the possibility of using angular cuts to isolate the new physics contribution from the SM background at a fixed energy, a strategy

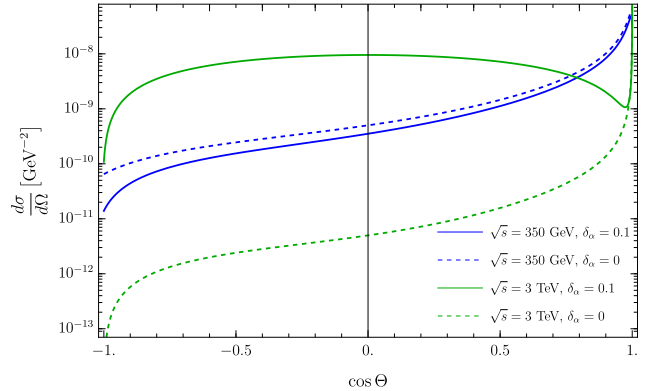


FIG. 3. The angular distribution of the differential cross section at two fixed energies:  $\sqrt{s} = 350$  GeV (blue solid line: including the NP contribution with  $\delta_\alpha = 0.1$ , blue dashed line: SM result) and  $\sqrt{s} = 3$  TeV, corresponding to the center of mass energies of FCC-ee and CLIC (green solid line: including the NP contribution with  $\delta_\alpha = 0.1$ , green dashed line: SM result).

that is described in ref. [8], where an analogous study of the effects of violation of unitarity in the quark mixing matrix is presented. The effectiveness of this strategy is illustrated in Fig. 3 for the benchmarks of FCC-ee and CLIC discussed above. Evidently, in the high energy regime where the cross section is dominated by the unitarity-violating terms, an angular cut centered around the scattering angle  $\Theta = \pi/2$  would enhance the effects of PMNS unitarity violation, so that deviations from the SM prediction are more easily detected in this angular region.

## V. UNITARITY TESTS AT HADRON COLLIDERS

Present and future hadron colliders can use the same method to probe the unitarity of the PMNS matrix by means of the inverse process

$$pp \rightarrow \ell_\alpha^+ \ell_\alpha^- jj, \quad \alpha = e, \mu, \tau, \quad (42)$$

proceeding via a pair of  $W$  bosons produced from initial quarks, where on top of the charged lepton pair, two jets  $jj$  appear in the final state. The corresponding (partonic) Feynman diagrams are shown in Fig. 4.

To estimate the size of the cross section for this process, we resort to the Effective Vector Boson Approximation (EVBA) [41]. This computational scheme replaces the virtual  $W$  bosons emitted from the initial quark lines with real  $W$  vector bosons, emitted with probabilities that depend on whether they are longitudinally (L) or transversely (T) polarised. The related partonic square amplitude admits the same decomposition presented in Eq. (33) for leptonic initial states, but we need to distinguish among the initial  $WW$  polarisations. In particular,

for the  $W^+W^- \rightarrow \ell^+\ell^-$  process the square amplitude can be decomposed as

$$|M_{\text{ww}}^{AB}|^2 = |M_{\text{SM}}^{AB}|^2 + \delta_\alpha \Delta_1^{AB} + \delta_\alpha^2 \Delta_2^{AB} \quad (43)$$

where  $AB = \{LL, TT, LT\}$  indicate the different polarisation combinations and  $|M_{\text{SM}}^{AB}|^2$  denotes the SM con-

tribution [41, 42]. The expressions for the  $\Delta M_{1,2}^{AB}$  terms are given in Appendix B.

Using the results given in Ref. [43], we obtain for the differential distribution of the cross section as a function of invariant mass  $m_{\ell\ell}$  of the resulting lepton pair:

$$\frac{d\sigma}{dm_{\ell\ell}}(pp \rightarrow \ell^+\ell^-jj) = \int_{m_{\ell\ell}^2/S}^1 \frac{da}{\sqrt{a}} \sum_{q_1, q_2} L^{q_1 q_2}(z) \left[ L_{LL}(a) \sigma_{\text{ww}}^{LL}(m_{\ell\ell}^2) + L_{TT}(a) \sigma_{\text{ww}}^{TT}(m_{\ell\ell}^2) + L_{LT}(a) \sigma_{\text{ww}}^{LT}(m_{\ell\ell}^2) \right], \quad (44)$$

where  $L_{AB}$  are the  $WW$  luminosities for the  $AB = (LL), (TT), (LT)$  polarisations,  $\sigma_{\text{ww}}^{AB}(m_{\ell\ell})$  are the corresponding polarised cross sections for the  $W^+W^- \rightarrow \ell^+\ell^-$  process evaluated at the lepton-pair invariant mass, and the symbol  $L^{q_1 q_2}(z)$  denotes the differential parton luminosity for initial  $q_1 q_2$  quark state carrying a fraction

$z = m_{\ell\ell}^2/(aS)$  of the total center-of-mass energy square, while the sum extends over all pairs of  $u, d, s, c, b$  quarks and antiquarks that can produce a  $W^+W^-$  pair.<sup>5</sup>

In the limit where the initial quark energy is much above the  $W$  boson mass, the polarised  $WW$  luminosities [41] and the quark luminosities are given by

$$\begin{aligned} L_{LL}(a) &= -\left(\frac{\alpha_w}{4\pi}\right)^2 \frac{1}{a} [(1+a) \log a + 2(1-a)], \\ L_{TT}(a) &= -\left(\frac{\alpha_w}{8\pi}\right)^2 \frac{1}{a} [2(1-a)(3+a) + (2+a)^2 \log a] \left[ \log \left( \frac{m_{\ell\ell}^2}{a M_W^2} \right) \right]^2, \\ L_{LT}(a) &= \left(\frac{\alpha_w}{8\pi}\right)^2 \frac{1}{a} [-7 + 6a + a^2 - 4(1+a) \log a] \log \left( \frac{m_{\ell\ell}^2}{a M_W^2} \right), \\ L^{q_1 q_2}(z) &= 4 \sqrt{\frac{z}{S}} \int_z^1 \frac{dx}{x} f_{q_1}(x) f_{q_2} \left( \frac{z}{x} \right), \end{aligned} \quad (45)$$

where, with a slight abuse of notation,  $L_{LT}$  indicates the sum of both the  $L_{LT}$  and  $L_{TL}$  contributions, and  $f_{q_1}$  and  $f_{q_2}$  denote the parton distribution functions of quarks  $q_1$  and  $q_2$  inside the colliding proton pairs.

In order to assess the possibility offered by hadron colliders, in the following we again compare the cross section obtained for a non-vanishing value of  $\delta_\alpha$  to the SM case.

With respect to the cleaner case offered by lepton colliders, we expect that the presence of sizable backgrounds due to the  $Z$  boson or the photon, for instance, will inevitably worsen the reach of our methodology. Nevertheless, we point out that these machines offer a unique possibility for testing unitarity breaking effects involving  $\tau$  lepton pairs, which complement the results obtained at a lepton colliders using electron or muon initial states. Having said that, in this first exploratory analysis we

neglect the possible effects of certain background processes in gauging the reach of the upcoming HL phase of LHC [44, 45] and the FCC-hh collider, as for example the contribution of diagrams similar to the first one in fig. 4 with the  $W$  bosons replaced by  $Z$  bosons or photons, which would add incoherently to the  $jj\ell^+\ell^-$  production. In first approximation this is justified since the contribution from the  $Z$ -diagrams is suppressed with respect to the  $W^+W^-$  signal by the smaller  $Z\bar{q}q$  and  $Z\bar{\ell}\ell$  couplings [42], while the contribution from  $\gamma$  diagrams can be kept under control by selecting final states containing jets with sizable transverse momentum [46]. However, more refined estimates should not dispense with a dedicated treatment of these, as well as other, background processes, and should also account for detector effects specific to each experiment.

In order to derive the potential unitarity bounds that could be set by the high luminosity phase of LHC on  $\delta_\ell$ , we perform a  $\chi^2$  test as in Eq. (38), by considering the total cross section from Eq. (44) integrated in the range  $200 \text{ GeV} \leq m_{\text{ww}} \leq 1 \text{ TeV}$ . With the PDF4LHC21 PDFs given in Ref. [47] and setting  $\sqrt{S} = 13 \text{ TeV}$ , the HL-LHC

<sup>5</sup> The contributions of the  $c$  and  $b$ -quarks are strongly suppressed for the center of mass energy of the HL-LHC and, therefore, can be neglected in this setting. They must however be included when assessing the power of the upcoming FCC-hh experiment.

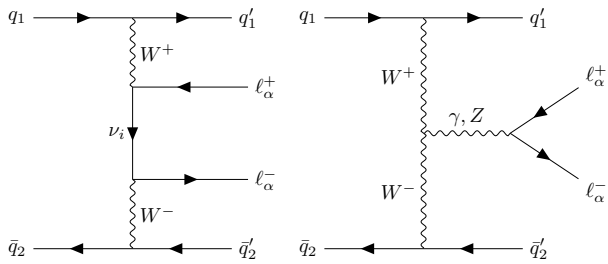


FIG. 4. Tree level Feynman diagrams for the processes  $pp \rightarrow jj \ell_\alpha^+ \ell_\alpha^-$ , ( $\alpha = e, \mu, \tau$ ). The arrows on the fermion lines indicate the momentum flow.

luminosity benchmark of  $\mathcal{L} = 3 \text{ ab}^{-1}$  [44] gives

$$\delta_\alpha < 1.0 \times 10^{-3} \quad (\text{HL-LHC, 95\% CL}), \quad (46)$$

for every flavor  $\alpha = e, \mu, \tau$ . Notice that the bound is flavor blind, being obtained in the massless-fermion limit and under the assumption that the background is given solely by the SM process  $W^+W^- \rightarrow \ell_\alpha^+ \ell_\alpha^-$ . As mentioned before, this constraint can thus also be applied to the  $\delta_\tau$  case, which is not accessible at lepton colliders.

We extend the analysis to assess the reach of the proposed method at the future circular hadron collider FCC-hh [48, 49], operating at  $\sqrt{S} = 100 \text{ TeV}$ . For the computation in Eq. (44) we again use the PDF4LHC21 PDFs given in Ref. [47], with  $\sqrt{S} = 100 \text{ TeV}$  and factorisation scale  $\hat{s} = zS$ . Using the  $\chi^2$  test as in Eq. (38), and considering the total cross section from Eq. (44) integrated over the range  $200 \text{ GeV} \leq m_{WW} \leq 9 \text{ TeV}$ , we obtain

$$\delta_\alpha < 4.4 \times 10^{-5} \quad (\text{FCC-hh, 95\% CL}) \quad (47)$$

for every lepton flavor  $\alpha = e, \mu, \tau$ , and ignoring, again, the effect of potential backgrounds.

## VI. CONCLUSIONS

We have proposed a strategy to probe the unitarity of the PMNS matrix using  $W$  boson pair production at collider experiments. At electron-positron and muon colliders, the key observable is the ratio of the  $\ell_\alpha^+ \ell_\alpha^- \rightarrow W^+W^-$  ( $\alpha = e, \mu$ ) cross section to its SM prediction: any non-zero value of the flavor-diagonal non-unitarity parameters  $\delta_\alpha$  spoils the gauge cancellation between  $s$ - and  $t$ -channel amplitudes, inducing an anomalous energy growth in the cross section at energies below the mass threshold of the new heavy states responsible for the loss of unitarity in the mixing matrix. At hadron colliders, the same effect can be investigated by analyzing the inverse process,  $pp \rightarrow W^+W^- \rightarrow \ell_\alpha^+ \ell_\alpha^- jj$  ( $\alpha = e, \mu, \tau$ ). Thus, our strategy enables hadron colliders to probe possible unitarity-violating effects in the  $\tau$  sector, which are inaccessible at experimental facilities based on electron or muon initial states.

Experiment	$\sqrt{s}$ [TeV]	$\mathcal{L}$ [ $\text{ab}^{-1}$ ]	Bound
FCC-ee	0.35	1.8	$\delta_e \lesssim 1.6 \times 10^{-4}$
ILC	1	8	$\delta_e \lesssim 9.6 \times 10^{-5}$
CLIC	3	5	$\delta_e \lesssim 9.1 \times 10^{-5}$
$\mu$ -collider BM1	3	1	$\delta_\mu \lesssim 2.2 \times 10^{-4}$
$\mu$ -collider BM2	10	10	$\delta_\mu \lesssim 3.1 \times 10^{-5}$
HL-LHC	13	3	$\delta_\alpha \lesssim 1.0 \times 10^{-3}$
FCC-hh	100	30	$\delta_\alpha \lesssim 4.4 \times 10^{-5}$

TABLE II. Summary of the bounds achievable by the different collider experiments. The bounds obtainable at hadron collider hold for all flavors  $\alpha = e, \mu, \tau$ .

The results obtained for the flavor-diagonal non-unitarity parameters at a 95% confidence level are summarised in Table II. Taken at face value, these bounds show that the proposed method can indeed complement, and potentially even outclass, the results of electroweak precision measurements especially in the electron and tau sectors. The extent to which loop corrections, background processes and detector effects will affect the proposed method will require a case-by-case dedicated study, which goes beyond the scope of this paper.

## Acknowledgments

It is a great pleasure to thank Emanuele Bagnaschi and Gennaro Corcella for insightful discussions in the early stages of this project. This work was supported by the Estonian Research Council grants TARISTU24-TK10, TARISTU24-TK3, RVTT3, and by the CoE TK 202 ‘‘Foundations of the Universe’’, and by the CERN Science Consortium of Estonia, grant RVTT3. The work of K.M. was supported by the Estonian Research Council grant PUTJD1256. The work of E.N. and L.M. was also supported by the Estonian Research Council team grant PRG1884.

### Appendix A

We provide below the complete analytical expressions for the quantities  $\Delta_{1,2}$  appearing in Eq. (33):

$$\begin{aligned} \Delta_1 = & \frac{4\alpha_w^2\pi^2}{(1-\beta_w^2)^2(1-2\beta_w c_\Theta + \beta_w^2)^2(M_Z^2 - s)} \left\{ s(1-\beta_w^2) \left[ -8 + 24\beta_w c_\Theta \right. \right. \\ & - \beta_w^2(7+9c_\Theta^2) - 16\beta_w^3 c_\Theta + 2\beta_w^4(7+3c_\Theta^2 + 2c_\Theta^4) - 8\beta_w^5 c_\Theta^3 - 3\beta_w^6(1-c_\Theta^2) \left. \right] \\ & + 2M_Z^2 \left[ 4 - 8\beta_w c_\Theta(2-s_w^2) + \beta_w^2(9+c_\Theta^2(11-13s_w^2) - 19s_w^2) \right. \\ & + 4\beta_w^3 c_\Theta(-1+12s_w^2+c_\Theta^2(1-2s_w^2)) - \beta_w^4(10+s_w^2+3c_\Theta^2(2+s_w^2) + 4c_\Theta^4(1-s_w^2)) \\ & + 4\beta_w^5 c_\Theta(3+c_\Theta^2-10s_w^2) + \beta_w^6(1+15s_w^2+4c_\Theta^4 s_w^2 - c_\Theta^2(5-13s_w^2)) \\ & \left. \left. - 8\beta_w^7 c_\Theta^3 s_w^2 - 3\beta_w^8(1-c_\Theta^2)s_w^2 \right] \right\}, \end{aligned} \quad (A1)$$

$$\begin{aligned} \Delta_2 = & \frac{4\alpha_w^2\pi^2}{(1-\beta_w^2)^2(1-2\beta_w c_\Theta + \beta_w^2)^2} \left[ 4 - 16\beta_w c_\Theta + \beta_w^2(9+11c_\Theta^2) - 4\beta_w^3 c_\Theta(1-c_\Theta^2) \right. \\ & \left. - 2\beta_w^4(5+3c_\Theta^2+2c_\Theta^4) + 4\beta_w^5 c_\Theta(3+c_\Theta^2) + \beta_w^6(1-5c_\Theta^2) \right]. \end{aligned} \quad (A2)$$

The definitions of the symbols appearing in Eqs. (A1)-(A2) can be found in section III.

### Appendix B

We list below the expressions for the unitarity-violation corrections to the polarised square amplitudes  $|M_{1,2}^{AB}|^2$  for the process  $W^+W^- \rightarrow \ell^+\ell^-$ , for the combinations of polarisation  $AB = \{LL, TT, LT\}$ :

$$\begin{aligned} \Delta_1^{LL} = & \frac{16\alpha_w^2\pi^2(1-c_\Theta^2)(\beta_w^3-3\beta_w+2c_\Theta)}{(1-\beta_w^2)^2(1+\beta_w^2-2\beta_w c_\Theta)^2(s-M_Z^2)} \left\{ s \left[ (1-\beta_w^2)(-3\beta_w+\beta_w^3+4c_\Theta-2\beta_w^2 c_\Theta) \right] \right. \\ & \left. - 2M_Z^2 \left[ 2c_\Theta - 3\beta_w(1-s_w^2) - \beta_w^5 s_w^2 - 6\beta_w^2 c_\Theta s_w^2 + 2\beta_w^4 c_\Theta s_w^2 + \beta_w^3(1+2s_w^2) \right] \right\}, \\ \Delta_2^{LL} = & \frac{16\alpha_w^2\pi^2(1-c_\Theta^2)(\beta_w^3-3\beta_w+2c_\Theta)^2}{(1-\beta_w^2)^2(1+\beta_w^2-2\beta_w c_\Theta)^2}, \\ \Delta_1^{TT} = & \frac{32\alpha_w^2\pi^2(1-c_\Theta^2)}{(1+\beta_w^2-2\beta_w c_\Theta)^2(s-M_Z^2)} \left\{ s \left[ 2 - \beta_w^4 - 3\beta_w c_\Theta + 3\beta_w^3 c_\Theta + 4c_\Theta^2 + \beta_w^2(1-2c_\Theta^2) \right] \right. \\ & \left. - 2M_Z^2 \left[ 1 + 2c_\Theta^2 - \beta_w c_\Theta(2-s_w^2) - \beta_w^4 s_w^2 + 3\beta_w^3 c_\Theta s_w^2 + \beta_w^2(1-s_w^2-2c_\Theta^2 s_w^2) \right] \right\}, \\ \Delta_2^{TT} = & \frac{32\alpha_w^2\pi^2(1-c_\Theta^2)(1+\beta_w^2-2\beta_w c_\Theta+2c_\Theta^2)}{(1+\beta_w^2-2\beta_w c_\Theta)^2}, \\ \Delta_1^{LT} = & -\frac{64\alpha_w^2\pi^2}{(1-\beta_w^2)(1+\beta_w^2-2\beta_w c_\Theta)^2(s-M_Z^2)} \left\{ s(1-\beta_w^2) \left[ -1 + 2\beta_w^3 c_\Theta + 3c_\Theta^2 + 6\beta_w c_\Theta^3 - 4c_\Theta^4 - \beta_w^2(1+5c_\Theta^2) \right] \right. \\ & + M_Z^2 \left[ 1 - 3c_\Theta^2 + 4c_\Theta^4 + \beta_w^4(1+c_\Theta^2(1-12s_w^2) - 4s_w^2) + 4\beta_w c_\Theta^3(s_w^2-2) + 4\beta_w^5 c_\Theta s_w^2 \right. \\ & \left. \left. + 4\beta_w^3 c_\Theta(3(1+c_\Theta^2)s_w^2-2) + 2\beta_w^2(1-2s_w^2-4c_\Theta^4 s_w^2 + c_\Theta^2(5-2s_w^2)) \right] \right\}, \\ \Delta_2^{LT} = & \frac{32\alpha_w^2\pi^2}{(1-\beta_w^2)(1+\beta_w^2-2\beta_w c_\Theta)^2} \left\{ 1 - 8\beta_w^3 c_\Theta - 3c_\Theta^2 - 8\beta_w c_\Theta^3 + 4c_\Theta^4 + \beta_w^4(1+c_\Theta^2) + 2\beta_w^2(1+5c_\Theta^2) \right\}. \end{aligned} \quad (B1)$$

- [1] B. Pontecorvo, “Inverse Beta Processes and Nonconservation of Lepton Charge,” *Sov. Phys. JETP* **7** (1958) 172–173.
- [2] Z. Maki, M. Nakagawa, and S. Sakata, “Remarks on the unified model of elementary particles,” *Prog. Theor. Phys.* **28** (1962) 870–880.
- [3] D. V. Forero, S. Morisi, M. Tortola, and J. W. F. Valle, “Lepton flavor violation and non-unitary lepton mixing in low-scale type-I seesaw,” *JHEP* **09** (2011) 142, [arXiv:1107.6009 \[hep-ph\]](#).
- [4] L. Basso, O. Fischer, and J. J. van der Bij, “Precision tests of unitarity in leptonic mixing,” *EPL* **105** no. 1, (2014) 11001, [arXiv:1310.2057 \[hep-ph\]](#).
- [5] S. Antusch and O. Fischer, “Non-unitarity of the leptonic mixing matrix: Present bounds and future sensitivities,” *JHEP* **10** (2014) 094, [arXiv:1407.6607 \[hep-ph\]](#).
- [6] E. Nardi, E. Roulet, and D. Tommasini, “Limits on neutrino mixing with new heavy particles,” *Phys. Lett. B* **327** (1994) 319–326, [arXiv:hep-ph/9402224](#).
- [7] S. Antusch, C. Biggio, E. Fernandez-Martinez, M. B. Gavela, and J. Lopez-Pavon, “Unitarity of the Leptonic Mixing Matrix,” *JHEP* **10** (2006) 084, [arXiv:hep-ph/0607020](#).
- [8] E. Gabrielli, L. Marzola, and K. Mürsepp, “Testing the CKM unitarity at high energy via the  $W+W-$  production at the LHC and future colliders,” *Phys. Lett. B* **859** (2024) 139106, [arXiv:2405.14585 \[hep-ph\]](#).
- [9] P. Minkowski, “ $\mu \rightarrow e\gamma$  at a Rate of One Out of  $10^9$  Muon Decays?,” *Phys. Lett. B* **67** (1977) 421–428.
- [10] T. Yanagida, “Horizontal gauge symmetry and masses of neutrinos,” *Conf. Proc. C* **7902131** (1979) 95–99.
- [11] R. N. Mohapatra and G. Senjanovic, “Neutrino Mass and Spontaneous Parity Nonconservation,” *Phys. Rev. Lett.* **44** (1980) 912.
- [12] M. Gell-Mann, P. Ramond, and R. Slansky, “Complex Spinors and Unified Theories,” *Conf. Proc. C* **790927** (1979) 315–321, [arXiv:1306.4669 \[hep-th\]](#).
- [13] S. F. King, “Large mixing angle MSW and atmospheric neutrinos from single right-handed neutrino dominance and  $U(1)$  family symmetry,” *Nucl. Phys. B* **576** (2000) 85–105, [arXiv:hep-ph/9912492](#).
- [14] S. F. King, “Constructing the large mixing angle MNS matrix in seesaw models with right-handed neutrino dominance,” *JHEP* **09** (2002) 011, [arXiv:hep-ph/0204360](#).
- [15] P. H. Frampton, S. L. Glashow, and T. Yanagida, “Cosmological sign of neutrino CP violation,” *Phys. Lett. B* **548** (2002) 119–121, [arXiv:hep-ph/0208157](#).
- [16] J. A. Casas and A. Ibarra, “Oscillating neutrinos and  $\mu \rightarrow e, \gamma$ ,” *Nucl. Phys. B* **618** (2001) 171–204, [arXiv:hep-ph/0103065](#).
- [17] T. Hambye, Y. Lin, A. Notari, M. Papucci, and A. Strumia, “Constraints on neutrino masses from leptogenesis models,” *Nucl. Phys. B* **695** (2004) 169–191, [arXiv:hep-ph/0312203](#).
- [18] A. Ibarra, E. Molinaro, and S. T. Petcov, “Low Energy Signatures of the TeV Scale See-Saw Mechanism,” *Phys. Rev. D* **84** (2011) 013005, [arXiv:1103.6217 \[hep-ph\]](#).
- [19] R. N. Mohapatra and J. W. F. Valle, “Neutrino Mass and Baryon Number Nonconservation in Superstring Models,” *Phys. Rev. D* **34** (1986) 1642.
- [20] R. N. Mohapatra, “Mechanism for Understanding Small Neutrino Mass in Superstring Theories,” *Phys. Rev. Lett.* **56** (1986) 561–563.
- [21] G. Anamiati, M. Hirsch, and E. Nardi, “Quasi-Dirac neutrinos at the LHC,” *JHEP* **10** (2016) 010, [arXiv:1607.05641 \[hep-ph\]](#).
- [22] E. K. Akhmedov, M. Lindner, E. Schnapka, and J. W. F. Valle, “Left-right symmetry breaking in NJL approach,” *Phys. Lett. B* **368** (1996) 270–280, [arXiv:hep-ph/9507275](#).
- [23] E. K. Akhmedov, M. Lindner, E. Schnapka, and J. W. F. Valle, “Dynamical left-right symmetry breaking,” *Phys. Rev. D* **53** (1996) 2752–2780, [arXiv:hep-ph/9509255](#).
- [24] A. Herrero-Brocal and A. Vicente, “Minimal Majorana neutrino mass models,” [arXiv:2510.00113 \[hep-ph\]](#).
- [25] J. H. García, S. Marcano, J. Racker, and D. Vatsyayan, “The Generalised Casas-Ibarra Parametrisation for Majorana Neutrino Masses,” [arXiv:2510.18962 \[hep-ph\]](#).
- [26] H. Hettmansperger, M. Lindner, and W. Rodejohann, “Phenomenological Consequences of sub-leading Terms in See-Saw Formulas,” *JHEP* **04** (2011) 123, [arXiv:1102.3432 \[hep-ph\]](#).
- [27] W. Alles, C. Boyer, and A. J. Buras, “ $W$  Boson Production in  $e^+e^-$  Collisions in the Weinberg-Salam Model,” *Nucl. Phys. B* **119** (1977) 125–140.
- [28] M. Lemoine and M. J. G. Veltman, “Radiative Corrections to  $e^+e^- \rightarrow W^+W^-$  in the Weinberg Model,” *Nucl. Phys. B* **164** (1980) 445–483.
- [29] R. Philippe, “ $W^-$  Pair Production in Electron - Positron Annihilation,” *Phys. Rev. D* **26** (1982) 1588.
- [30] M. Bohm, A. Denner, T. Sack, W. Beenakker, F. A. Berends, and H. Kuijff, “Electroweak Radiative Corrections to  $e^+e^- \rightarrow W^+W^-$ ,” *Nucl. Phys. B* **304** (1988) 463–499.
- [31] F. Behner, “ $WW$  and  $ZZ$  production at LEP,” *PoS silafae-III* (2000) 003.
- [32] FCC Collaboration, A. Abada *et al.*, “FCC-ee: The Lepton Collider: Future Circular Collider Conceptual Design Report Volume 2,” *Eur. Phys. J. ST* **228** no. 2, (2019) 261–623.
- [33] FCC Collaboration, M. Benedikt *et al.*, “Future Circular Collider Feasibility Study Report: Volume 1, Physics, Experiments, Detectors,” [arXiv:2505.00272 \[hep-ex\]](#).
- [34] ILC Collaboration, “The International Linear Collider Technical Design Report - Volume 2: Physics,” [arXiv:1306.6352 \[hep-ph\]](#).
- [35] P. Bambade *et al.*, “The International Linear Collider: A Global Project,” [arXiv:1903.01629 \[hep-ex\]](#).
- [36] ILC International Development Team Collaboration, A. Aryshev *et al.*, “The International Linear Collider: Report to Snowmass 2021,” [arXiv:2203.07622 \[physics.acc-ph\]](#).
- [37] “Physics and Detectors at CLIC: CLIC Conceptual Design Report,” [arXiv:1202.5940 \[physics.ins-det\]](#).
- [38] CLIC Collaboration, J. de Blas *et al.*, “The CLIC Potential for New Physics,” *CERN Yellow Rep. Monogr.* **3** (2018) 1–282, [arXiv:1812.02093 \[hep-ph\]](#).

- [39] O. Brunner *et al.*, “The CLIC project,” [arXiv:2203.09186](#) [[physics.acc-ph](#)].
- [40] **International Muon Collider** Collaboration, C. Accettura *et al.*, “Interim report for the International Muon Collider Collaboration (IMCC),” *CERN Yellow Rep. Monogr.* **2/2024** (2024) 176, [arXiv:2407.12450](#) [[physics.acc-ph](#)].
- [41] S. Dawson and S. S. D. Willenbrock, “Heavy Fermion Production in the Effective  $W$  Approximation,” *Nucl. Phys. B* **284** (1987) 449.
- [42] D. A. Dicus, “Exact Calculation of Heavy Lepton Production From  $WW$  Fusion,” *Nucl. Phys. B* **287** (1987) 397–401.
- [43] D. Green, “ $W^+W^- \rightarrow ZZ$  scattering at the LHC,” [arXiv:hep-ex/0309031](#).
- [44] I. B. Alonso, O. Brüning, P. Fessia, M. Lamont, and L. Rossi, eds., *High-Luminosity Large Hadron Collider (HL-LHC): Technical Design Report*. CERN Yellow Reports: Monographs. 2020.
- [45] O. B. *et al.*, *LHC Design Report*. CERN, 2004.
- [46] B. E. Cox, A. De Roeck, V. A. Khoze, T. Pierzchala, M. G. Ryskin, I. Nasteva, W. J. Stirling, and M. Tasevsky, “Detecting the standard model Higgs boson in the  $WW$  decay channel using forward proton tagging at the LHC,” *Eur. Phys. J. C* **45** (2006) 401–407, [arXiv:hep-ph/0505240](#).
- [47] **PDF4LHC Working Group** Collaboration, R. D. Ball *et al.*, “The PDF4LHC21 combination of global PDF fits for the LHC Run III,” *J. Phys. G* **49** no. 8, (2022) 080501, [arXiv:2203.05506](#) [[hep-ph](#)].
- [48] “Physics at the FCC-hh, a 100 TeV pp collider,” [arXiv:1710.06353](#) [[hep-ph](#)].
- [49] **FCC** Collaboration, A. Abada *et al.*, “FCC Physics Opportunities: Future Circular Collider Conceptual Design Report Volume 1,” *Eur. Phys. J. C* **79** no. 6, (2019) 474.